Microbiology (2007), **153**, 3124–3132 DOI 10.1099/mic.0.2007/007625-0

Nanomechanical properties of glucans and associated cell-surface adhesion of *Streptococcus mutans* probed by atomic force microscopy under *in situ* conditions

Sarah E. Cross,[1,3]† Jens Kreth,[4]† Lin Zhu,[4] Richard Sullivan,[6] Wenyuan Shi,[4,5] Fengxia Qi[4] and James K. Gimzewski[1,3]

Correspondence
James K. Gimzewski
gim@chem.ucla.edu

[1]UCLA Department of Chemistry and Biochemistry, Los Angeles, CA 90095, USA
[2]UCLA California NanoSystems Institute, Los Angeles, CA 90025, USA
[3]UCLA Institute for Cell Mimetic Space Exploration, Los Angeles, CA 90095, USA
[4]UCLA School of Dentistry, Los Angeles, CA 90095, USA
[5]UCLA Molecular Biology Institute, Los Angeles, CA 90095, USA
[6]Colgate-Palmolive, Piscataway, NJ 08855, USA

This study used atomic force microscopy (AFM) to probe the local cell-surface interactions associated with the glucan polymers of *Streptococcus mutans*, the macromolecules most commonly attributed to the virulence of this microbe. *In situ* force spectroscopy was used to quantitatively probe and correlate cell-surface adhesion and dynamics with *S. mutans* UA140 wild-type and five glucosyltransferase mutants. Adhesion between the tooth surface and *S. mutans* is largely mediated by glucan production from sucrose via three glucosyltransferases (Gtfs; GtfB, GtfC and GtfD). To monitor the contribution of these particular Gtfs, isogenic mutants of *S. mutans* were constructed by specific gene inactivation and compared to the wild-type under sucrose and non-sucrose conditions. We report direct measurement of the mechanical properties associated with glucan macromolecules demonstrating that the local adhesion strength increases in a time-dependent process, with a decrease in the average number of rupture events. This finding suggests that *S. mutans* attaches mainly through glucans to surfaces in the presence of sucrose. In addition, a possible role of the Gtf proteins in sucrose-independent attachment is supported by the decreased adhesion properties of the GtfBCD mutant compared to the wild-type.

Received 27 February 2007
Revised 3 May 2007
Accepted 9 May 2007

INTRODUCTION

Bacteria have a natural tendency to colonize surfaces in nature as well as in industrial and clinical settings through assembling multicellular communities via cell–cell and cell–surface interactions (Costerton *et al.*, 1995; O'Toole *et al.*, 2000). These bacterial communities are of particular medical importance due to their increased tolerance to antibiotics (Costerton *et al.*, 1999). With the formation of biofilms such as those produced by *Streptococcus mutans* (commonly referred to as dental plaque), cell–surface interactions play an enormous role in initial cell colonization, and cell–cell protein interactions largely mediate the growth and continued existence of biofilms (O'Toole *et al.*, 2000). The surface features of micro-organisms, such as those associated with *S. mutans*, are involved in most of the inter- and intra-species interactions. They play an important role during contact with the environment, organic and inorganic surfaces, as well as host organisms, and thus are pivotal for biofilm formation, virulence and metabolic regulation (Ghuysen & Hackenbeck, 1994).

The function, structure and properties of bacterial cell surfaces are determined by the presence of species-specific proteins, lipids and polysaccharides. Lactic-acid-producing bacteria like *S. mutans*, *Streptococcus sobrinus* and *Leuconostoc mesenteroides* produce specific exopolysaccharides called glucans, which constitute a major feature of the surface of these micro-organisms (Cerning, 1990). Glucans are chemically and physically complex high-molecular-mass homo-polysaccharides composed of a main linear chain of α-D-glucopyranose subunits. Several different kinds of glucans are known; they are categorized by the

†These authors contributed equally to this paper.

Abbreviations: AFM, atomic force microscopy; Gtf, glucosyltransferase.

 2007/007625 © 2007 SGM *Printed in Great Britain*

sizes and structures of the molecules: e.g. dextrans are principally linked through α(1-6) glucosidic bonds, and mutans through α(1-3) glucosidic bonds. Glucans are also distinguished by their degree of branching, the types of branch linkage [α(1-2), α(1-3), α(1-4) and α(1-6)], the extent of branch chains and the spatial arrangement (Cerning, 1990; Monchois *et al.*, 1999).

S. mutans is known as the principal dental pathogen associated with caries (Loesche, 1986). One of the most important virulence factors of *S. mutans* is the synthesis of glucan from sucrose (Hamada & Slade, 1980). Glucan synthesis allows the bacteria to firmly attach to the tooth surface and form a biofilm, while the gelatinous nature of glucan retards diffusion of acid produced by the bacteria from fermentable sugars in the dental plaque (Kuramitsu, 1993). This eventually leads to dissolution of the hard enamel surface of the tooth and cavity formation. Research on dental plaque development and the aetiology of dental caries has established the central role of glucans in sucrose-dependent adhesion, and the correlation between sucrose consumption and increased caries rates (Yamashita *et al.*, 1993; Loesche, 1986). In *S. mutans* these glucans are synthesized from sucrose by the action of three types of glucosyltransferases (Gtfs): GtfB and GtfC synthesize mainly water-insoluble glucans (>85 %) with α(1-3) glucosidic bonds (mutan); GtfD forms water-soluble glucans (>70 %) with α(1-6) glucosidic bonds (dextran) (Monchois *et al.*, 1999). The contribution of the individual glucans to the cariogenicity has been the subject of several studies, including the identification and characterization of the enzymes and genes encoding the respective Gtfs and showing that the action of all Gtfs is essential for the maximal cellular adherence (Tsumori & Kuramitsu, 1997). Ooshima *et al.* (2001) demonstrated that the maximal sucrose-dependent adherence can be achieved by adding recombinant Gtfs to *S. mutans* in a ratio of 5 rGtfB : 0.25 rGtfC : 1 rGtfD. However, most of these studies were conducted under non-physiological conditions or with isolated recombinant proteins.

We chose *S. mutans*, a biologically and medically relevant bacterial species, to investigate the role that glucans play in the virulence of this organism. The detailed knowledge about the genetic organization of the *gtf* genes enabled us to construct strains with individual mutations of these genes. The biochemical and biophysical properties of microbial surfaces resulting from the enzymic activity of Gtfs have been extensively studied in numerous bacterial species using techniques such as dynamic light scattering and micro-electrophoresis which require intense manipulation of the cell surface as well as lengthy preparation of the cell (Cerning, 1990; Ryan *et al.*, 1980). However, *in vivo* techniques such as atomic force microscopy (AFM) (Binnig *et al.*, 1986) provide a novel, nondestructive method for providing insight into critical properties associated with bacterial cells and their related surface proteins. AFM has proved to be a powerful tool not only for imaging of the ultrastructure of bacterial surfaces under *in situ* conditions, but also for determining the associated mechanical properties and intermolecular forces (Pelling *et al.*, 2005; Rief *et al.*, 1997). Schär-Zammaretti & Ubbink (2003a, b) probed the surface properties of different *Lactobacillus* strains using AFM to quantify tip–cell-surface adhesion forces and related this study to the ability of the lactobacilli to adhere to surfaces, clustering, auto- and co-aggregation. van der Mei *et al.* (2000) used AFM to determine cellular stiffness of fibrillated and non-fibrillated strains of *Streptococcus salivarius*.

Cross *et al.* (2006) demonstrated that the surface roughness of *S. mutans* strains harbouring genetic mutations of specific surface proteins correlated with their different cariogenic potential. Together with the mechanical analysis of the cell-surface protein interactions, these studies clearly demonstrate the potential use of AFM for characterization of bacterial surface properties under physiological conditions using intact bacterial cells. As these studies were conducted with uncompromised cells under *in situ* conditions, the results add substantial new information regarding the cell-adhesion and cariogenic properties of *S. mutans* and the individual role of the Gtfs in its adhesion properties. Here we report direct measurement of the mechanical properties associated with the cell-surface macromolecules native to *S. mutans* wild-type and mutant strains as probed by AFM.

METHODS

Strains and growth conditions. *S. mutans* strain UA140 (Qi *et al.*, 2001) and its derivatives were grown in Todd–Hewitt (TH, Difco) medium or on brain heart infusion (BHI, Difco) agar plates. For selection of antibiotic-resistant colonies, BHI plates were supplemented with 800 μg kanamycin ml^{-1}, 15 μg erythromycin ml^{-1} or 5 μg tetracycline ml^{-1} (Sigma). All *S. mutans* strains were grown anaerobically (80 % N_2, 10 % CO_2 and 10 % H_2) at 37 °C. For cloning and plasmid amplification, *Escherichia coli* cells were grown in Luria–Bertani (LB, Fisher) medium with aeration at 37 °C. *E. coli* strains carrying plasmids were grown in LB medium supplemented with 25 μg kanamycin ml^{-1}.

Construction of various Gtf$^-$ mutants. The GtfBCD$^-$, GtfBC$^-$ and GtfD$^-$ mutant strains were constructed by transferring the particular mutations of *gtfBC* (Erm^R) and *gtfD* (Tet^R) combined or individually into UA140 (kindly provided by H. Kuramitsu, University of Buffalo, NY, USA). Plasmid and chromosomal DNA was transformed into *S. mutans* after induction of an exponential culture with a synthetic competence-stimulating peptide (CSP, 1 μg ml^{-1}) (Kreth *et al.*, 2005) for 2 h with the subsequent addition of DNA. After further incubation for 2–3 h the culture was plated on selective media. To generate the *gtfB* deletional mutant, two fragments corresponding to approximately 1 kb of upstream and downstream sequence of the target gene were generated by PCR using *Pfu* and *Taq* polymerase mix (2 : 1 ratio) and the primers gtfB upF (5′-GCTAGCGAGAAGATTGCTG-AGCGATC-3′), gtfB upR (5′-ATAGTCTGACGCAGCCAATC-3′), gtfB downF (5′-TGGTCTACAGCTCAGAGATG-3′) and gtfB downR (5′-ATGAAGCAACAGATACTGTC-3′). These fragments were cloned into pGEM-T Easy (Promega). All plasmids were extracted and purified from *E. coli*, digested with appropriate restriction enzymes, gel-purified and ligated to compatible restriction sites of the erythromycin-resistance cassette and the cloning plasmid

pBluescript (Stratagene). The *gtfC* deletional mutant was created by using the same protocol, except that the primers for generating up- and downstream fragments were gtfC upF (5′-TGGAGAACGA-GTTCGGATTAAC-3′), gtfC upR (5′-TGACTAAGTGATGACG-GCTGTT-3′), gtfC downF (5′-TGTTCAGGCTAAGGGAGAGC-3′) and gtfC downR (5′-CCCATTTGTCGGCTTTTCTA-3′). The fragments were ligated with a kanamycin-resistance cassette and the cloning plasmid pBluescript through compatible restriction sites. The resulting plasmids were confirmed via restriction digestion as well as PCR and linearized for transformation into *S. mutans*. Transformants were selected on Erm plates for *gtfB* deletional mutant and on Kan plates for *gtfC* deletional mutant. Correct mutants were confirmed by PCR and their altered ability to form biofilms with sucrose compared to the parental strain.

Immobilization of *S. mutans* cells for AFM analysis. Two millilitres of an overnight culture in BHI medium (5×10^8 bacteria ml^{-1}) with no antibiotic added, supplemented with 1 % sucrose when indicated, were filtered through an isopore polycarbonate membrane (Millipore) with a pore size of 0.6 μm (i.e. slightly smaller than the diameters of streptococcal cells) to immobilize the bacteria through mechanical trapping, a common technique used to gather AFM images and force measurements of molecular interactions at microbial surfaces (Kasas & Ikai, 1995; Pelling *et al.*, 2004). After filtering, the filter was carefully removed from the filter device and fixed with double-sided tape onto a small Petri dish; 5 ml 50 % (v/v) BHI was added to the dish prior to imaging the sample using AFM, submerging the filter in liquid.

AFM methodology. All imaging in fluid was conducted using a Nanoscope IV Bioscope (Veeco Digital Instruments) (Fig. 1A). AFM images were collected in contact mode using sharpened silicon nitride cantilevers (OTR4 Veeco probes) with experimentally determined spring constants of 0.02 N m^{-1} and a nominal tip radius of <20 nm as defined by the manufacturer (Veeco). Probes were kept in their sterile original container as prepared using standard manufacturing techniques (Veeco), examined optically for debris before use and used promptly. Fluid imaging and mechanical measurements were obtained at room temperature (~20 °C), with force measurements recorded at a pulling rate of 1 Hz and the tip taken to be a conical indenter. Height and deflection images were simultaneously acquired; these are both important with regard to microbial cell surface characterization as they yield complementary information. Force–distance measurements were collected on single mechanically trapped *S. mutans* cells by lowering the cantilever tip toward the cell, pressing against the cell surface and retracting the tip from the cell as shown schematically in Fig. 1(D). The resulting curves, generated from the cantilever displacement, were analysed to reveal the force magnitude and relative cell surface adhesion by monitoring the rupture events revealed in the associated tip retraction traces from the cell surface (Fig. 1D) (Smith *et al.*, 1999). The force-spectroscopy analysis of the wild-type and mutant cells consisted of 100 measurements made on three individual cells in each case (n=300).

RESULTS

Analysis of local cell–surface interactions associated with the glucan polymers of *S. mutans* using *in situ* AFM

Individual strains of *S. mutans* were probed using AFM to determine the role of glucans in cell adhesion and aggregation of *S. mutans* (Fig. 1), thus yielding quantitative information regarding the mechanics of these glucan-polymer macromolecules. Kreth *et al.* (2004) demonstrated that the concentration of 1 % sucrose during growth as a static culture is in a saturating range for maximal biofilm adhesion strength. We report results for 1 % sucrose-treated cells compared to control, untreated cells in our experiments. To determine the right time point for probing of *S. mutans* cells by AFM, we compared cells grown without sucrose to those supplemented with 1 % sucrose at the exponential growth phase (6 h) and at the stationary phase (12 h). Fig. 2 shows the results obtained with *S. mutans* UA140 wild-type cells. These cells were mechanically trapped, and under a liquid environment (see Methods) force–displacement curves were collected on the cells. The applied force of the tip against the cell was ~5 nN. With retraction of the tip from the cell wall a sequence of rupture events was observed, forming sawtooth-like patterns (Fig. 3) revealing the nature of the adhesive interactions between the local cell-surface macromolecules and the AFM tip (Fisher *et al.*, 2000; Sen *et al.*, 2005). In addition, force curves taken on the bare substrate, before and after cellular measurements, showed no rupture events, indicating null adhesion and confirming no contamination of the AFM tip, which may have otherwise caused nonspecific tip–cell-surface binding (Fig. 3). As shown in Table 1, the mean rupture force for *S. mutans* UA140 wild-type control, 6 h and 12 h sucrose-treated cells was 84.1 ± 156.0, 304.3 ± 281.9 and 375.6 ± 563.2, respectively. A two-sample independent t test was conducted on the mean rupture force obtained for the control, 6 h and 12 h sucrose-treated cases. At the 95 % confidence level, it was found that the population mean for *S. mutans* UA140 wild-type control cells was significantly different from both the population means for the 6 h and 12 h sucrose-treated conditions ($P \leqslant 0.00001$). However, the population means for *S. mutans* UA140 wild-type cells after 6 h and 12 h of sucrose treatment were not significantly different. Interestingly, the number of observed events (noe) for the wild-type control cells (noe=6705) was significantly higher than the number observed for the sucrose-treated samples at both time points (noe=88 for 6 h sucrose-treated cells; noe=261 for 12 h sucrose-treated cells) (Fig. 2). The large number of unbinding events observed in the case of the wild-type control cells is most likely due to the presence of several surface proteins, such as Pac and Wap (Bowen *et al.*, 1991; Russell *et al.*, 1995), which under non-sucrose conditions may cause increased tip–cell-surface interactions, whereas after sucrose is introduced into the system glucan chain growth induces tip–cell-surface protein interactions at a tip–cell distance significantly larger than that required for tip interactions with shorter surface proteins, thus yielding fewer overall adhesion events yet much stronger binding. Moreover, observed adhesion events for the sucrose-treated wild-type cells generally showed significantly increased tip-retraction lengths compared to those exhibited by the control cells (Fig. 3). Although variation in tip–cell contact regions play a part in resulting retraction lengths, the increase in retraction length observed for the sucrose-treated cells indicates that the cell-surface macromolecules on the sucrose-treated wild-type cells are generally longer than

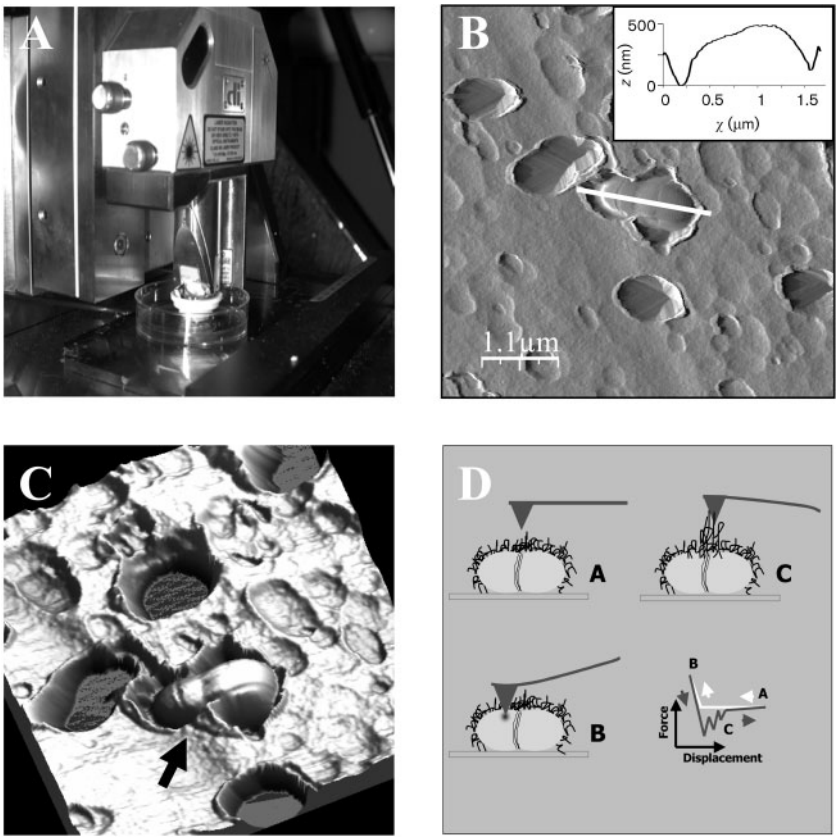

Fig. 1. (A) Image of mounted AFM head with fluid tip holder and mounted cantilever submerged in medium over mechanically trapped cells. (B) AFM deflection-mode image of a mechanically trapped *S. mutans* wild-type cell in fluid; the inset shows the height profile corresponding to the white line drawn along the long axis of the mechanically trapped cell. (C) 3D rendering of an AFM height-mode image of the area in B (cell indicated by the arrow); image scan size 4 μm. (D) Schematic representation of an AFM tip interacting with cell-surface macromolecules: A, before tip-cell interaction; B, tip pushing into cell surface; C, tip pulling away from cell surface. The force–displacement curve (bottom right) corresponds to the tip–cell images A–C.

those of the non-sucrose-treated cells. Together these results indicate that the optimum adhesion for these cells is in the stationary phase, as the sucrose is most likely used up by the cells for the synthesis of the glucan polymers and metabolic purposes.

Associated cell-surface adhesion of five Gtf mutants of *S. mutans* observed using AFM under physiological conditions

In addition to obtaining adhesion forces for *S. mutans* UA140 wild-type cells before (control) and after treatment with sucrose (12 h) we examined the effect of sucrose on five different *S. mutans* UA140 mutant strains which had individual mutations in specific *gtf* genes. The cell shapes of these mutants did not differ significantly from each other or the wild-type as shown by the series of representative AFM deflection-mode images of wild-type and mutant cells under both sucrose and non-sucrose conditions in Fig. 4. Force–displacement curves were collected on *S. mutans* UA140 *gtfB*, *gtfC*, *gtfD*, *gtfBC* and *gtfBCD* mutant strains under non-sucrose and sucrose conditions. As shown in Table 1, the mean rupture force observed for UA140 *gtfB* control cells was 46.1 ± 80.6 pN. After treatment with sucrose for 12 h the mean rupture force increased to 53.0 ± 148.3 pN for this mutant strain. The average unbinding force obtained for UA140 *gtfC* cells before and after treatment with sucrose for 12 h was 42.0 ± 28.5 and 43.9 ± 68.8 pN, respectively (Table 1). Similarly the control mean unbinding force for UA140 *gtfD* mutant cells was 42.7 ± 22.4 pN; however, the mean unbinding force after treatment with sucrose for 12 h increased significantly to 111.3 ± 128.2 pN (Table 1). Such an increase in the observed mean adhesion force, compared to the other mutant strains, is expected since the GtfD$^-$ strain is still able to produce water-insoluble glucans. Control and sucrose-treated mean unbinding forces for *S. mutans* UA140 *gtfBC* cells were 35.1 ± 22.4 pN and 53.2 ± 46.0 pN, respectively. With mutation of three specific genes, *gtfBCD*, the measured average adhesion remained consistently low in both the control and sucrose-treated cases, yielding values of 36.3 ± 17.3 and 37.4 ± 14.2 pN, respectively (Table 1). These observations were anticipated, as mutation of three specific *gtf* genes is known to abolish sucrose-dependent colonization (Tsumori & Kuramitsu, 1997). Data collected on all cell types were obtained using different tip–cell combinations and provided consistent results in all cases.

Observed rupture forces for *S. mutans* UA140 *gtfB* and *gtfC* mutant strains as compared to the wild-type

In addition to the average rupture force required to break the bonds between the AFM tip and the surface proteins of the cell, the number of observed rupture events provides

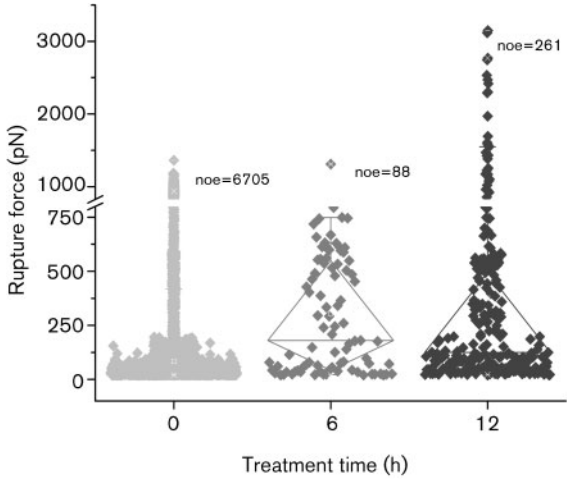

Fig. 2. Box-whisker plot of the observed rupture force between the AFM tip and *S. mutans* UA140 wild-type cells. The data represent the unbinding force observed due to tip–cell adhesion for three individual cells at each treatment time (0, 6 and 12 h). The average rupture force for the wild-type cells in each case, untreated control (0 h), 6 h and 12 h sucrose-treated is 84 ± 156, 304 ± 282 and 376 ± 563 pN, respectively ($P \leqslant 0.00001$ for control vs both 6 h and 12 h). The force-spectroscopy analysis of these cells consisted of 100 measurements made on three individual cells in each case. Note the similarity in the number of observed events (noe) in the 6 h and 12 h treated cells as compared with the much higher number of observed events seen in the untreated cells.

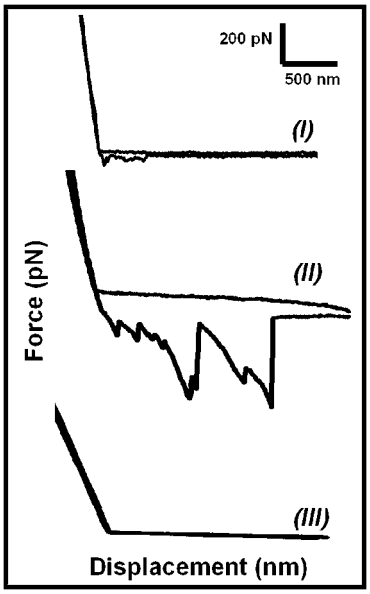

Fig. 3. Force–displacement curves measured on *S. mutans* UA140 wild-type cells: typical force curves collected for (*I*) control and (*II*) 12 h sucrose-treated cells. Force–displacement curves were collected for approach and retraction of the AFM tip against the cell surface. Regions of the cell surface were visualized topographically via AFM before obtaining force curves on the surface to ensure consistency of the local cell-surface area for each cell and cell type analysed. Rupture events, exhibiting a sawtooth-like pattern, are visible in both the control and 12 h sucrose-treated cases; however, the corresponding force of adhesion between the tip and cell surface is significantly increased in wild-type cells exposed to sucrose conditions for 12 h (curve *II*). (*III*) A typical force–displacement curve measured on the substrate after force-spectroscopy measurements were performed on a *S. mutans* wild-type cell.

insight into the nature of these surface proteins. In particular, we were interested in analysing the change in observed rupture events for *S. mutans* UA140 *gtfB* and *gtfC* mutant strains as compared to the wild-type. Both GtfB and GtfC produce similar glucans but they seem to have different importance in the adhesion process as shown by the force–displacement curves. The percentage of rupture force events occurring in particular force regions was calculated for *S. mutans* UA140 wild-type, *gtfB* and *gtfC* cells under both sucrose and non-sucrose conditions (Table 2). Interestingly, the data indicate a significant shift in the percentage of tip–cell-surface rupture events occurring at lower-range forces under both sucrose and non-sucrose conditions for the wild-type as compared with the mutant strains. For example, at a rupture force of 20 ± 5 pN the percentage of observed events for the wild-type cells was ~28 % when untreated and ~9 % when treated with sucrose; however, the percentage of observed events for both UA140 *gtfB* and *gtfC* was significantly greater, with observed values of ~68 % for *gtfB* and ~38 % for *gtfC* under non-sucrose conditions and ~52 % for both mutants under sucrose conditions (Table 2). Moreover, at higher-range forces the percentage of observed tip–cell-surface rupture events increased for the wild-type in the presence of glucose. The direct comparison between the overall increase in rupture events between $GtfB^-$ (possessing GtfC and GtfD activity) and $GtfC^-$ (possessing GtfB and GtfD activity) reveals that the $GtfB^-$ mutant is still able to increase sucrose- vs non-sucrose-mediated events, although the increase is not as strong as seen in the wild-type (data not shown).

DISCUSSION

S. mutans is able to utilize sucrose to synthesize α(1-3) and α(1-6) glucosidic polymers and form a biofilm on surfaces such as tooth enamel, plastic and glass (Hamada & Slade, 1980; Kreth *et al.*, 2004). The purpose of this study was to determine the contribution of the individual glucan-polymers to molecular-level interfacial properties of this micro-organism, such as cell adhesion. We have used AFM (Rief *et al.*, 1997) to probe the mechanics of these macromolecules. AFM has become a pivotal imaging technique for the ultrastructure of bacterial surfaces under

Table 1. Summary of mean rupture force with associated SD and median values obtained from force–displacement curves collected on *S. mutans* UA140 wild-type and mutant cells

gtfBCD is used to denote the Gtf genes *gtfB*, *gtfC* and *gtfD*. WT, wild-type; $n=300$.

Strain	Control (no sucrose)			6 h sucrose			12 h sucrose		
	Mean (pN)	SD (±pN)	Median	Mean (pN)	SD (±pN)	Median	Mean (pN)	SD (±pN)	Median
wt	84.1	156.0	39.0	304.3	281.9	194.2	375.6	563.2	124.7
gtfB	46.1	80.6	25.3	–	–	–	53.0	148.3	35.4
gtfC	42.0	28.5	33.8	–	–	–	43.9	68.8	29.4
gtfD	42.7	22.4	36.0	–	–	–	111.3	128.2	48.6
gtfBC	35.1	22.4	28.0	–	–	–	53.2	46.0	37.3
gtfBCD	36.3	17.3	31.0	–	–	–	37.4	14.2	32.3

in vivo and *in situ* conditions and has been used to determine the mechanical properties and molecular forces of bacterial cells (Cross *et al.*, 2006; Schär-Zammaretti & Ubbink, 2003a, b; van der Mei *et al.*, 2000; Zhu *et al.*, 2006). The force-measuring aspect of AFM unveils the inter- and intra-molecular forces (van der Aa *et al.*, 2001) through recording the force–displacement curves as illustrated by the schematic in Fig. 1(D). An AFM probe is brought close to the cell surface, indented into the cell surface, and then retracted from the surface. Macromolecules, such as glucan-polymers, attach to the tip during extension of the probe towards the cell surface. The piezoelectric transducer retracts the probe from the cell surface, causing an extension of the attached macromolecule(s) as the tip–cell distance is increased. The force required to separate the probe from the cell-surface molecules is determined by the bending of the AFM cantilever (Morris *et al.*, 2004). Upon separation of the tip and cell-surface macromolecules, rupture events occur, often forming sawtooth-like patterns representative of the sequential stretching, unfolding and breakage of the cell-surface macromolecules, thus revealing the adhesive nature of the biomolecules native to the cell surface (Fig. 1D). Mechanical properties of macromolecules at the microbial surface are commonly probed by studying the tip–cell interactions observed in force spectroscopy experiments (van der Aa *et al.*, 2001). Tip–cell-surface transient and local interactions serve as a reasonable model for probing adhesive properties at the surface of microbial cells (Pelling *et al.*, 2005; van der Aa *et al.*, 2001; Zhu *et al.*, 2006). This

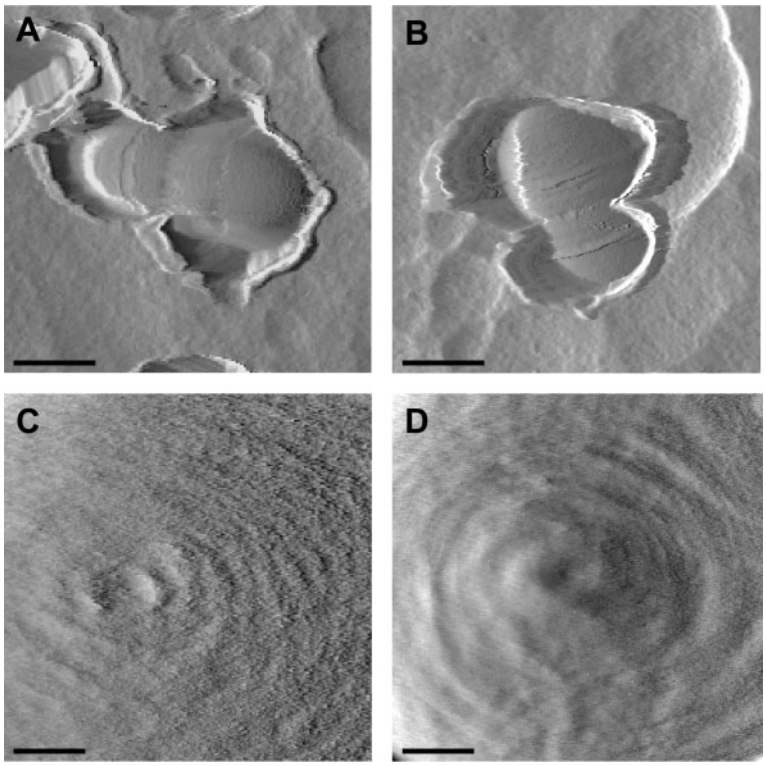

Fig. 4. Typical AFM deflection-mode images of representative *S. mutans* wild-type and mutant cells under non-sucrose (control) and sucrose conditions (12 h). (A) *In situ*, mechanically trapped *S. mutans* wild-type cell grown without sucrose, (B) single GtfC$^-$ cell grown with sucrose, (C) section of a single trapped GtfC$^-$ cell grown without sucrose, (D) analogous section of a GtfBC$^-$ cell grown with sucrose. Scale bars: A, B, 500 nm; C, D, 60 nm.

Table 2. Percentage of rupture events observed at selected unbinding force regions for *S. mutans* UA140 wild-type, *gtfB* and *gtfC* mutant cells under non-sucrose (−) and sucrose (+) conditions

The data are from 100 force curves, collected at 12 h, on three individual cells in each case. (Note: GtfB$^-$ possesses GtfC and D activty and GtfC$^-$ possesses GtfB and D activity. WT, wild-type; n=300.)

Rupture force (pN)	Rupture force events (%)					
	WT		GtfB$^-$		GtfC$^-$	
	(−)	(+)	(−)	(+)	(−)	(+)
20±5	28.34	9.20	67.56	51.81	38.33	51.76
80±5	2.71	3.83	0.99	3.43	0.63	0.27
140±5	0.40	0.77	0.50	0.29	1.04	0.27
190±5	0.09	1.92	0.30	0.38	0.21	0.27
1170±5	0.05	0.77	0	0	0	0
2740±5	0	0.38	0	0	0	0
3140±5	0	0.38	0	0	0	0

technique has commonly been applied to measure forces associated with DNA, polysaccharides and proteins (Pelling *et al.*, 2005; Rief *et al.*, 1997; van der Aa *et al.*, 2001).

Although AFM has garnered much interest in the last decade due to its ability to successfully probe the morphological and mechanical properties of living cells, there still remain some limitations with the technique. For example, sample preparation, cantilever flexibility and speed are significant aspects of AFM that need to be addressed to aid in further understanding of cellular structure–function. The soft and elastic propeties of live cell surfaces still remain problematic for obtaining atomic- or nanometre-resolution images; moreover, immobilization of the live cell is critical for examination by AFM. The current state of AFM allows measurement of biological processes *in situ*; however, an increase of scanning speed with less applied force is desirable for reliably examining biological phenomena in real time. Introduction of increasingly fine, less damaging and less sticky probes remains to be addressed by manufacturers. Despite these limitations, AFM remains one of the best techniques for high-resloution, low-force, quantitative analysis of live cells. Thus, we have used AFM to probe one of the most important virulence factors of *S. mutans*, its ability to synthesize glucans from sucrose via three Gtfs. Using the force spectroscopy component of AFM we were able to quantify the mechanics associated with particular cell-surface macromolecules, glucans, for *S. mutans* UA140 wild-type and isogenic mutant strains under physiological conditions.

Tip–cell-surface transient and local interactions were analysed for information elucidating the adhesive properties associated with *S. mutans* UA140 wild-type and *gtf* mutant strains. Our findings indicate, as expected, that the wild-type cells exhibit increased adhesion as compared to the mutant strains. Furthermore, when cells are grown for 12 h in the presence of sucrose the average local adhesion strength increases dramatically. However, the average number of observed rupture events for *S. mutans* wild-type significantly decreased when cells were exposed to sucrose as compared to the non-sucrose-treated cells. These findings indicate that the glucan macromolecule chains present on the cell surface undergo significant growth when cells are exposed to sucrose for a prolonged period. It appears that the lengthy glucan chains form tip–cell-surface interactions further away from the cell surface; thus the number of unbinding events decreases in the presence of longer glucan chains as interference with the tip occurs at an earlier stage than that caused by cell-surface macromolecules similar to those noted in the control cells. Thus, the attachment of *S. mutans* to the enamel surface of the tooth in the presence of sucrose may be mediated exclusively by the synthesized glucans. Furthermore, the observed decline in the number of rupture events is accompanied by a dramatic increase in the overall adhesion strength, thus suggesting a more uniform surface structure. Consistent with this observation is the downregulation of expression of the *wapA* gene, encoding the surface protein WapA, in the presence of sucrose. The surface properties of a WapA$^-$ mutant, clearly distinguishable when grown without sucrose, become similiar to the wild-type when cells are grown in the presence of sucrose (Zhu *et al.*, 2006). Once the sucrose-independent attachment process is completed, *S. mutans* can switch to a stronger adhesion via glucans when sucrose becomes available.

Interestingly, the AFM method used revealed a possible additional feature of the Gtfs. When comparing the mean rupture force for the wild-type to that of the triple mutant UA140 *gtfBCD* (84.1 pN vs 36.3 pN) it becomes evident that the proteins themselves contribute to the adhesion between the cell surface and the cantilever tip. Although the cantilever material is different from the tooth surface, this suggests that the enzymes could be involved in the initial attachment of the cell to the tooth surface.

Furthermore, previous studies have demonstrated that the three Gtfs are required to promote full adhesion to the tooth surface (Tsumori & Kuramitsu, 1997). However, the extent to which the Gtfs contribute to the adhesion varies. GtfC seems to play a more prominent role in the adhesion event, as demonstrated by the heterologous expression of Gtfs in *Streptococcus milleri*. Only GtfC was able to promote significant sucrose-dependent attachment to smooth surfaces (Fukushima *et al.*, 1992). This result was further supported in an *in vitro* biofilm model by Tsumori & Kuramitsu (1997). In our results, the strain expressing GtfC and GtfD (UA140 *gtfB*) showed a slight increase in the mean rupture forces in the presence of sucrose, while the strain expressing GtfB and GtfD (UA140 *gtfC*) showed an insignificant increase in the mean rupture

forces. The GtfC- and GtfD-expressing strain was still able to adhere to a glass test tube, whereas the GtfB- and GtfD-expressing strain failed to adhere (data not presented). These results suggest that the broader distribution of rupture events in the GtfB$^-$ mutant, as shown by the relatively high standard deviation, is important for attachment (53.0 ± 148.3 pN vs 43.9 ± 68.8 pN in the GtfC$^-$ mutant). Future work employing functionalized tips may be useful for further analysis of the contribution to adhesion made by each individually expressed Gtf. The coating of a functionalized tip with saliva could change curve characteristics, as shown for *S. mutans* strain ATCC 25175 (van Hoogmoed *et al.*, 2006).

The method used to probe *S. mutans* cells under the conditions described may not detecting solely the interactions of the cantilever tip with the glucans, but also with additional proteins associated with the glucans. A well-described group of proteins interacting with glucans are the glucan-binding proteins or Gbps. Four different types of Gbps (GbpA to GbpD) have been identified in *S. mutans*. Some of them are involved in biofilm morphology and cell aggregation (Banas & Vickerman, 2003). Of particular interest for this study is the binding ability of GbpC to the water-soluble glucan synthesized by GtfD (Matsumoto *et al.*, 2006). The GtfD mutant is still able to adhere to glass and showed a mean rupture force of 111.3 pN. This is about threefold less than the wild-type. However, the GtfBC$^-$ mutant only expressing GtfD could not adhere to the glass surface and the mean rupture force did not increase substantially after sucrose addition. This suggests that the water-soluble glucans somehow require the presence of the water-insoluble glucans to provide full adhesion. If this binding is mediated by GbpC then the role of GbpC as well as the role of the other Gbps in sucrose-dependent adhesion needs to be addressed in future research.

ACKNOWLEDGEMENTS

This work was supported in part by NIH grants U01-DE15018 to W. S., R01-DE014757 to F. Q., and a Delta Dental grant WDS78956 to W. S.; S. E. C. and J. K. G. acknowledge partial support from the Colgate-Palmolive Company: Application of Nanotechnology to Oral Care.

REFERENCES

Banas, J. A. & Vickerman, M. M. (2003). Glucan-binding proteins of the oral streptococci. *Crit Rev Oral Biol Med* **14**, 89–99.

Binnig, G., Quate, C. F. & Gerber, C. (1986). Atomic force microscope. *Phys Rev Lett* **56**, 930–933.

Bowen, W. H., Schilling, K., Giertsen, E., Pearson, S., Lee, S. F., Bleiweis, A. & Beeman, D. (1991). Role of a cell surface-associated protein in adherence and dental caries. *Infect Immun* **59**, 4606–4609.

Cerning, J. (1990). Exocellular polysaccharides produced by lactic acid bacteria. *FEMS Microbiol Rev* **7**, 113–130.

Costerton, J. W., Lewandowski, Z., Caldwell, D. E., Korber, D. R. & Lappin-Scott, H. M. (1995). Microbial biofilms. *Annu Rev Microbiol* **49**, 711–745.

Costerton, J. W., Stewart, P. S. & Greenberg, E. P. (1999). Bacterial biofilms: a common cause of persistent infections. *Science* **284**, 1318–1322.

Cross, S. E., Kreth, J., Zhu, L., Qi, F. X., Pelling, A. E., Shi, W. Y. & Gimzewski, J. K. (2006). Atomic force microscopy study of the structure-function relationships of the biofilm-forming bacterium *Streptococcus mutans*. *Nanotechnology* **17**, S1–S7.

Fisher, T. E., Marszalek, P. E. & Fernandez, J. M. (2000). Stretching single molecules into novel conformations using the atomic force microscope. *Nat Struct Biol* **7**, 719–724.

Fukushima, K., Ikeda, T. & Kuramitsu, H. K. (1992). Expression of *Streptococcus mutans gtf* genes in *Streptococcus milleri*. *Infect Immun* **60**, 2815–2822.

Ghuysen, J. M. & Hackenbeck, R. (1994). *Bacterial Cell Wall*. Amsterdam: Elsevier.

Hamada, S. & Slade, H. D. (1980). Biology, immunology, and cariogenicity of *Streptococcus mutans*. *Microbiol Rev* **44**, 331–384.

Kasas, S. & Ikai, A. (1995). A method for anchoring round shaped cells for atomic force microscope imaging. *Biophys J* **68**, 1678–1680.

Kreth, J., Hagerman, E., Tam, K., Merritt, J., Wong, D. T., Wu, B. M., Myung, N. V., Shi, W. & Qi, F. (2004). Quantitative analyses of *Streptococcus mutans* biofilms with quartz crystal microbalance, microjet impingement and confocal microscopy. *Biofilms* **1**, 277–284.

Kreth, J., Merritt, J., Shi, W. & Qi, F. (2005). Co-ordinated bacteriocin production and competence development: a possible mechanism for taking up DNA from neighbouring species. *Mol Microbiol* **57**, 392–404.

Kuramitsu, H. K. (1993). Virulence factors of mutans streptococci: role of molecular genetics. *Crit Rev Oral Biol Med* **4**, 159–176.

Loesche, W. J. (1986). Role of *Streptococcus mutans* in human dental decay. *Microbiol Rev* **50**, 353–380.

Matsumoto, M., Fujita, K. & Ooshima, T. (2006). Binding of glucan-binding protein C to GTFD-synthesized soluble glucan in sucrose-dependent adhesion of *Streptococcus mutans*. *Oral Microbiol Immunol* **21**, 42–46.

Monchois, V., Willemot, R. M. & Monsan, P. (1999). Glucansucrases: mechanism of action and structure-function relationships. *FEMS Microbiol Rev* **23**, 131–151.

Morris, S., Hanna, S. & Miles, M. J. (2004). The self-assembly of plant cell wall components by single-molecule force spectroscopy and Monte Carlo modelling. *Nanotechnology* **15**, 1296–1301.

O'Toole, G., Kaplan, H. B. & Kolter, R. (2000). Biofilm formation as microbial development. *Annu Rev Microbiol* **54**, 49–79.

Ooshima, T., Matsumura, M., Hoshino, T., Kawabata, S., Sobue, S. & Fujiwara, T. (2001). Contributions of three glycosyltransferases to sucrose-dependent adherence of *Streptococcus mutans*. *J Dent Res* **80**, 1672–1677.

Pelling, A. E., Sehati, S., Gralla, E. B., Valentine, J. S. & Gimzewski, J. K. (2004). Local nanomechanical motion of the cell wall of *Saccharomyces cerevisiae*. *Science* **305**, 1147–1150.

Pelling, A. E., Li, Y., Shi, W. & Gimzewski, J. K. (2005). Nanoscale visualization and characterization of *Myxococcus xanthus* cells with atomic force microscopy. *Proc Natl Acad Sci U S A* **102**, 6484–6489.

Qi, F., Chen, P. & Caufield, P. W. (2001). The group I strain of *Streptococcus mutans*, UA140, produces both the lantibiotic mutacin I and a nonlantibiotic bacteriocin, mutacin IV. *Appl Environ Microbiol* **67**, 15–21.

Rief, M., Gautel, M., Oesterhelt, F., Fernandez, J. M. & Gaub, H. E. (1997). Reversible unfolding of individual titin immunoglobulin domains by AFM. *Science* **276**, 1109–1112.

Russell, M. W., Harrington, D. J. & Russell, R. R. (1995). Identity of *Streptococcus mutans* surface protein antigen III and wall-associated protein antigen A. *Infect Immun* **63**, 733–735.

Ryan, V., Hart, T. R. & Schiller, R. (1980). Laser light scattering measurement of dextran-induced *Streptococcus mutans* aggregation. *Biophys J* **31**, 113–125.

Schär-Zammaretti, P. & Ubbink, J. (2003a). Imaging of lactic acid bacteria with AFM–elasticity and adhesion maps and their relationship to biological and structural data. *Ultramicroscopy* **97**, 199–208.

Schär-Zammaretti, P. & Ubbink, J. (2003b). The cell wall of lactic acid bacteria: surface constituents and macromolecular conformations. *Biophys J* **85**, 4076–4092.

Sen, S., Subramanian, S. & Discher, D. E. (2005). Indentation and adhesive probing of a cell membrane with AFM: theoretical model and experiments. *Biophys J* **89**, 3203–3213.

Smith, B. L., Schaffer, T. E., Viani, M., Thompson, J. B., Frederick, N. A., Kindt, J., Belcher, A., Stucky, G. D., Morse, D. E. & Hansma, P. K. (1999). Molecular mechanistic origin of the toughness of natural adhesives, fibres and composites. *Nature* **399**, 761–763.

Tsumori, H. & Kuramitsu, H. (1997). The role of the *Streptococcus mutans* glucosyltransferases in the sucrose-dependent attachment to smooth surfaces: essential role of the GtfC enzyme. *Oral Microbiol Immunol* **12**, 274–280.

van der Aa, B. C., Michel, R. M., Asther, M., Zamora, M. T., Rouxhet, P. G. & Dufrene, Y. F. (2001). Stretching cell surface macromolecules by atomic force microscopy. *Langmuir* **17**, 3116–3119.

van der Mei, H. C., Busscher, H. J., Bos, R., de Vries, J., Boonaert, C. J. & Dufrene, Y. F. (2000). Direct probing by atomic force microscopy of the cell surface softness of a fibrillated and nonfibrillated oral streptococcal strain. *Biophys J* **78**, 2668–2674.

van Hoogmoed, C. G., Dijkstra, R. J. B., van der Mei, H. C. & Busscher, H. J. (2006). Influence of biosurfactant on interactive forces between mutans streptococci and enamel measured by atomic force microscopy. *J Dent Res* **85**, 54–58.

Yamashita, Y., Bowen, W. H., Burne, R. A. & Kuramitsu, H. K. (1993). Role of the *Streptococcus mutans gtf* genes in caries induction in the specific-pathogen-free rat model. *Infect Immun* **61**, 3811–3817.

Zhu, L., Kreth, J., Cross, S. E., Gimzewski, J. K., Shi, W. Y. & Qi, F. X. (2006). Functional characterization of cell-wall-associated protein WapA in *Streptococcus mutans*. *Microbiology* **152**, 2395–2404.

Edited by: P. E. Kolenbrander